

## STIRRED FLUIDIZED-BED DRYER OF REGENERATED ION EXCHANGER PARTICLES

MICHAL PĚNIČKA, PAVEL HOFFMAN\*, IVAN FOŘT

*Czech Technical University in Prague, Department of Process Engineering, Technická 4, 166 07 Prague, Czech Republic*

\* corresponding author: [pavel.hoffman@fs.cvut.cz](mailto:pavel.hoffman@fs.cvut.cz)

**ABSTRACT.** This paper describes the intensification of the fluidized-bed drying process for regenerated spherical-shape ion exchanger particles in batch mode, achieved by a mechanical stirrer in the fluidized bed layer of dried particles. The effect of the mechanical stirring system on the drying process is examined. The calculations and also the results of comparative measurements provide evidence of a favourable effect of stirring on the total drying time in comparison with the initial unstirred system. The regenerated ion exchanger particles pass to the fluid state in a shorter time and the ultimate total drying time is thus more than 60% shorter.

**KEYWORDS:** fluidized-bed drying; stirring; mechanical disruption; drying kinetics; ion exchanger.

### 1. INTRODUCTION

This study seeks savings in fluidized-bed drying of particles in batch mode, the particles being highly adhesive due to the surface tension of the liquid adhering to the particles. Drying is an extremely energy-demanding process, and so it is important – especially now that energy prices are becoming so high – to find ways to achieve energy savings. Fluidized-bed drying is a drying process in which intensive heat and mass transfer occur between the particles that are present in the fluid state and the air flowing through the bed. The surface tension of the liquid adhering to the surface of the particles at the beginning of the drying process gives rise to a strong tendency for the particles to stick to each other and also to the walls of the drying chamber. The batch mode of this process together with the insufficient amount of material present in a batch does not allow a vibro-fluid dryer to be used, since these dryers are mainly designed for continuous mode. A solution may be found in drying with a fluidized bed layer which is stirred [1–4] and where the particle clusters are disintegrated continuously and the particles adhering to the drying chamber walls are swept off due to the stirring process.

The aim of this study is to intensify and improve the drying process of the regenerated ion exchanger particles, i.e. to shorten the process while at the same time improving the homogeneity of the humidity of the particles.

### 2. MATERIAL AND METHODS

#### 2.1. SPHERICAL PARTICLES OF THE REGENERATED ION EXCHANGER

Ion exchanger particles are used in membrane technology processes for wastewater treatment purposes [5]. They are also widely used for water treatment in the nuclear power sector [6].

Ion exchangers are mostly synthetic high-molecular-weight organic compounds, largely based on styrene, polyacrylate, phenol formaldehyde resins, etc. [7]. The Marathon-A cation exchanger, consisting of spherical particles 450–580  $\mu\text{m}$  in diameter, was selected as the model material [8]. The maximum permitted temperature is 120°C to avoid thermal stress resulting in structural degradation of the particles.

The drying process consists of three main periods, see Fig. 1. In the initial phase (period 0-1 in Fig. 1), the particles act as a stationary porous layer. This period is characterized by particle surface moisture, resulting in a strong tendency toward adhesion. In their appearance and in their physical properties, the dried particles resemble an amorphous material (Fig. 2, point 0) and stick strongly to the walls and also to each other. The initial moisture of the regenerated ion exchanger is approximately 65% RM (Fig. 1). In this period the heat supplied by the drying air is used to evaporate the free surface water from the particles (Fig. 2, point 0). Thus the particle diameter remains constant in this period, as is clear from the particle diameter change curve during the drying process (see Fig. 1B). Due to imperfect circumfluence of the drying air around the particles (it flows through the layer only in several channels) the heat energy is not consumed completely, and thus both the drying air temperature and the humidity at the fluid chamber output are not close to the ideal state, i.e. the drying air humidity approaches the saturation limit and the temperature approaches the wet or moist bulb temperature (Fig. 1D, E).

As soon as the attractive forces from the water surface tension decrease enough to enable transition of the particles to the fluidized state (period 1–2 in Fig. 1), moisture starts to evaporate from the particles (Fig. 2, point 1). This transition to the fluidized state improves the drying air circumfluence of the particles and

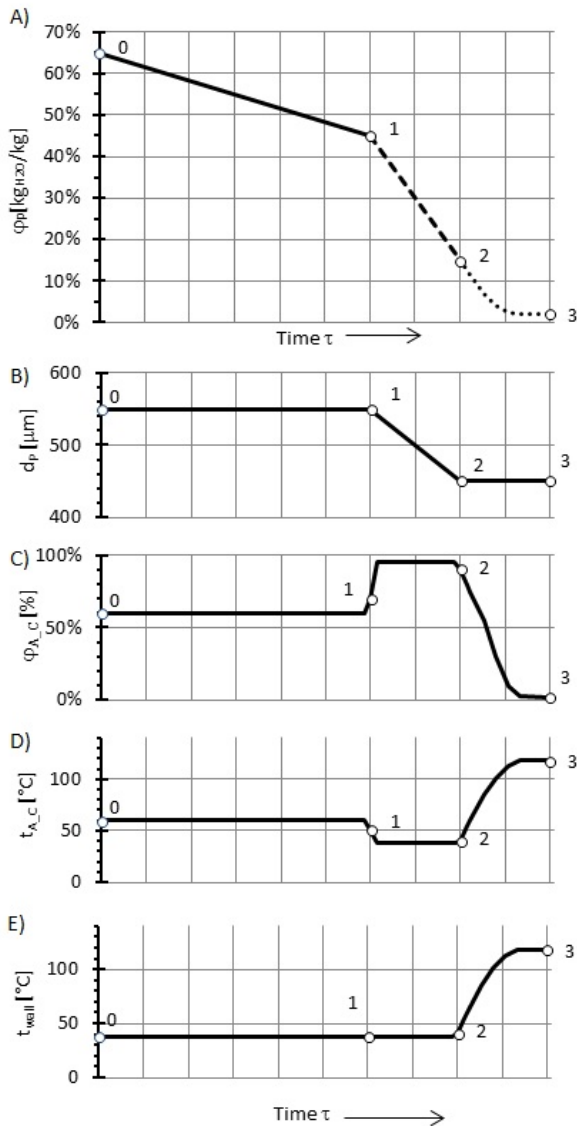


FIGURE 1. Time dependences of the particle and drying air properties during the whole drying process.

consequently accelerates the heat and also the mass transfer. As a result, the drying air temperature at the fluid chamber output starts to approach the wet bulb temperature, and the maximum possible humidity of the drying air is reached (Fig. 1C, D). The dried particles now get to what is referred to as the first drying period, in which the drying rate is constant. This material is characterized by a significant expansion in volume, depending on the moisture content of the material (Fig. 2, point 2). For this reason, the particle diameters are decreased in this period. The rate of moisture evaporation from the particle surface is lower than the rate of moisture transfer from the centre of the particle to the surface. Thus the limiting factor of the drying process is the evaporation from the particle surface.

After passing point 2 in Fig. 1, the diameter of the particles remains constant and the particles start to be dried to the required final moisture level. Through this

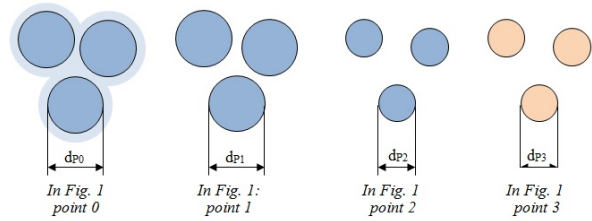


FIGURE 2. Particle diameter change curve during the drying process.

effect, the drying process reaches the second drying period, in which the drying rate decreases. The drying air temperature at the fluid chamber output increases and the humidity decreases. Moisture transfer from the particle centre to the surface is the limiting factor in this period.

## 2.2. STIRRING UNIT

The main issue in this process is that the particles stick to each other or to the dryer walls in the first drying period. This is caused by the surface tension of the liquid, which is present both on the surface and inside the particles. Hence, the properties of the stirrer are an important factor in the technology and in intensifying the process.

A suitable stirrer should have the capacity to disrupt the ion exchanger particle clusters and sweep the particles off the walls. This ability should be effective enough to minimise the initial drying period in which the particles adhere to each other, but not to cause particle degradation. The effect of the stirrer in the first and second periods, in which the surface of the pre-dried particles is dry enough for the particles to pass to the fluidized state, must not be adverse, i.e. it must not disturb the fluidized bed layer or the contact between the particles and the drying air, which would slow down the heat and mass transfer effects.

## 2.3. EXPERIMENTAL EQUIPMENT

An experimental equipment assembly for fluidized-bed drying with a stirred layer and various fluid chamber diameters was designed to evaluate the development of the drying process. The layout of the experimental equipment is shown in Fig. 3. Pressurized air at a known temperature and humidity is fed in from the main air distribution line (Fig. 3, item 1). The air flow is controlled by the pressure control valve (Fig. 3, Item 2) and is measured using a rotameter (Fig. 3, item 3). Downstream of the flowmeter the air is heated by a heating device with resistance wires, and the output of the unit is controlled manually by the voltage change using a transformer (Fig. 3, Item 4). The temperature of the heated air is measured upstream of the fluid chamber using a contact thermometer with accuracy of  $\pm 0.1^\circ\text{C}$ . The fluidized bed chamber (Fig. 3, item 5) consists of a duct made of a galvanized zinc sheet which is thermally isolated. This main part is 1 m

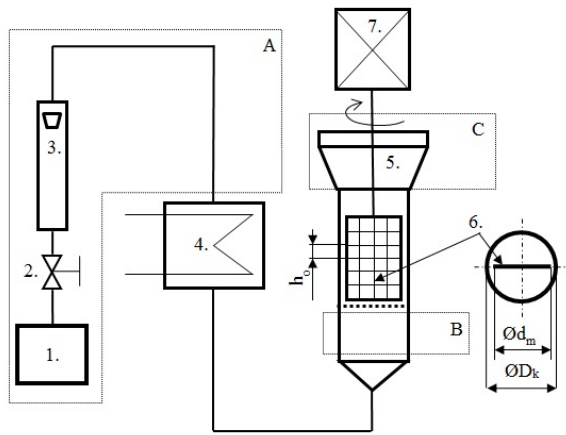


FIGURE 3. Experimental equipment layout.

long, and then the diameter is expanded to 250 mm. A sensor measuring the humidity of the drying air (accuracy  $\pm 0.1\%$ ) and the temperature of the drying air (accuracy  $\pm 0.1\%$ ) after passing the fluidized bed layer was positioned always 300 mm above the fluidized-bed chamber grid. This sensor is designed to determine the properties of the drying air at the output (point C in Fig. 4). An adjustable-speed stirrer unit is positioned above the chamber (Fig. 3, item 7).

A schematic drawing of the wire stirrer is shown in item 6 in Fig. 3. Fluidized bed chambers with three basic diameters (85 mm, 100 mm and 140 mm) were designed to enable the development of the model drying process to be precisely monitored.

**2.4. PROPERTIES OF THE DRYING AIR**

The flow rate of the heated air downstream of the heating unit was determined using the equation of state of an ideal gas (1), assuming that the amount of substance of the flowing air  $n_A$  at the heating unit input and output is constant, i.e. that there is no leakage of the drying air from the experimental equipment

$$p_A \dot{V}_A = n_A R T_A. \tag{1}$$

The values from points A and B in Fig. 4 are inserted in the equation of state, including the thermodynamic temperature of the drying air  $T_A$ , air pressure  $p_A$  and the universal gas constant  $R$ . The superficial drying air velocity  $u_{AB}$  of the drying chamber was determined from the air flow rate  $\dot{V}_A$  at the point B (Fig. 4)

$$u_{AB} = \frac{\dot{V}_A}{S_k}, \tag{2}$$

where  $S_k$  is the cross-section of the fluidized-bed chamber. The density of the wet air depending on the temperature was calculated according to equation (9)

$$\rho_A = \frac{1.316 \cdot 10^{-3}}{T_A} (2.65p + \varphi_A p''_V), \tag{3}$$

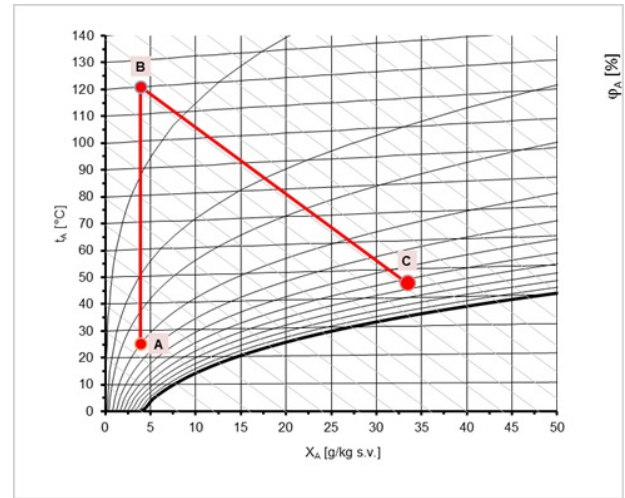


FIGURE 4. h-X diagram for the adiabatic drying process.

where  $\varphi_A$  is the relative humidity of the drying air and the pressure of the saturated water vapour  $p''_V$  at temperature  $T_A$  was determined according to relation (4), which is valid for the temperature range 0 to 200°C, where  $C_8$  to  $C_{13}$  are coefficients taken from the literature [10]

$$\ln p''_V = \frac{C_8}{T_A} + C_9 + C_{10}T_A + C_{11}T_A^2 + C_{12}T_A^3 + C_{13} \ln T_A. \tag{4}$$

The dependence of the dynamic viscosity of the drying air on temperature is expressed by equation (11)

$$\mu_A = 0.00004t_A + 0.176, \tag{5}$$

where  $t_A$  is the temperature of the drying air in degrees Celsius.

**2.5. DETERMINATION OF LAYER POROSITY**

Table 1 presents the values of the non-status initial conditions of the studied drying process of particles of the regenerated ion exchanger, identical for all tested sizes of the fluid drying chambers. The Reynolds number was determined from the known drying air velocity  $u_{AB}$  according to the equation

$$u_{AB} = \frac{Re \mu_A}{d_p \rho_A}, \tag{6}$$

where  $\mu_A$  is dynamic viscosity and  $\rho_A$  is density of the drying air. These values are determined according to equations (3) and (5). Variable  $d_p$  is the mean value of the particle diameter in the studied period. The relationship between porosity  $\varepsilon$  and drying air velocity  $u_{AB}$ , or between porosity and the Reynolds number  $Re$  is expressed [12] by an equation valid for fine particles:

$$Re = \frac{Ar \varepsilon^{4.75}}{18 + 0.6 \sqrt{Ar \varepsilon^{4.75}}}. \tag{7}$$

The Archimedes criterion  $Ar$  is determined according to the equation

$$Ar = \frac{d_p^3 (\rho_{SW} - \rho_A) \rho_A g}{\mu_A^2}, \tag{8}$$

Column diameter	$D_k$	m	0.085	0.100	0.140
Temperature of drying air at point B in Fig. 3	$t_A$	°C	120		
Density of drying air at point B in Fig. 3	$\varrho_A$	kg m <sup>-3</sup>	0.91		
Viscosity of drying air at point B in Fig. 3	$\mu_A$	Pa s	$2.24 \cdot 10^{-5}$		
Density of dry particles	$\varrho_s$	kg m <sup>-3</sup>	1440		
Superficial drying air velocity	$u_{AB}$	m s <sup>-1</sup>	2.1		

TABLE 1. Input parameters of the drying air.

where  $g$  is the acceleration of gravity and  $d_p$  is the mean particle diameter in the studied period.  $\varrho_A$  is the density and  $\mu_A$  is the dynamic viscosity of the drying air determined according to equations (3) and (5). The density of the wet particles  $\varrho_{SW}$  for the given interval is determined using the equation

$$\varrho_{SW} = \varrho_S \left( 1 + \frac{m_W}{m_S} \right), \quad (9)$$

where  $\varrho_S$  represents the density of the dried material and  $m_W$  is the mass of the liquid component of the corresponding moisture of the measured material at a given point in the studied process.

## 2.6. DETERMINING THE DRYING RATE

The drying rate is thus determined for the given interval according to equation [13]

$$- \frac{m_S}{A_S} \frac{\Delta X_W}{\Delta \tau} = N_W, \quad (10)$$

where  $\Delta X_W$  is the difference in absolute moisture between the initial and final point of the studied interval and  $\Delta \tau$  represents the drying period in the given period. The total particle surface was determined according to the formula

$$A_S = V_P a_S, \quad (11)$$

where the total particle volume  $V_P$  is calculated from the formula

$$V_P = \frac{m_S}{\varrho_{SW}}, \quad (12)$$

where  $m_S$  is the mass of the dry matter of the measured sample and  $\varrho_{SW}$  is the density of the wet particles for the given interval (9). The specific particle surface is determined according to the formula valid for monodisperse systems of spherical particles

$$a_s = \frac{6(1 - \varepsilon)}{d_p}, \quad (13)$$

where  $\varepsilon$  is the porosity in the studied period.

## 3. RESULTS AND DISCUSSION

### 3.1. DESIGN OF THE OPTIMIZED STIRRER FOR MINIMIZING THE TOTAL DRYING TIME

The Wire Stirrer prototype stirrer as shown schematically in Fig. 3, was designed on the basis of the results

of preliminary experiments with standardized stirrers. The stirrer is made of stainless steel wire 0.4 to 0.6 mm in diameter. It was designed for a centric arrangement. The diameter of the stirrer is 0.95–0.97  $d_m/D_k$  and its height is 2.8 to 5 times that of the material layer at rest. The expected rotation speed is approximately 50 rpm for all fluidized bed dryer sizes tested here. The peripheral speed of its blades is in the range of 0.225 to 0.26 ms<sup>-1</sup> for the column sizes tested.

The preliminary experiments clearly showed that when the stirrer mesh  $h_O$  is too small the wet ion exchanger particle clusters are insufficiently disintegrated and the clusters move along with it. If the stirrer mesh is too large, the particle clusters are disintegrated but the resulting clusters are not small enough. There was no significant effect of mesh orientation on the cluster disintegration process. The optimum mesh size was found to be 10 mm × 10 mm.

### 3.2. THE COURSE OF CHANGES IN ION EXCHANGER PARTICLE DIAMETERS IN THE TEST PERIODS

During individual experiments, samples of dried ion exchanger were taken every 5 minutes from the same point in the drying column. During the drying process, over 30 samples were taken for the unstirred version and over 13 samples for the stirred version. In a part of this sample, the absolute moisture of the sample was determined using drying balances. In this way, the moisture of the dried particles in a particular point of the drying process was determined. The rest of the sample was immediately subjected to microscopic analysis and photos of at least six particles were taken. The mean diameter of these particles for one particular point in the whole process of drying (and thus for the particular moisture of these particles) was then determined using an optical method. The average mean particle diameter value for all diameters of the columns, for the stirred and unstirred variants, was for the porous layer period  $d_{P_{01}} = 590 \cdot 10^{-6} \text{ m} \pm 2\%$ , for the first period of the fluidized-bed layer  $d_{P_{12}} = 530 \cdot 10^{-6} \text{ m} \pm 3\%$ , and for the second period of the fluidized-bed layer  $d_{P_{23}} = 460 \cdot 10^{-6} \text{ m} \pm 3\%$ . The dependence of the mean particle diameter value on the absolute moisture of the particle is shown in Fig. 5, where the transition points between individual periods in Fig. 1 are highlighted.

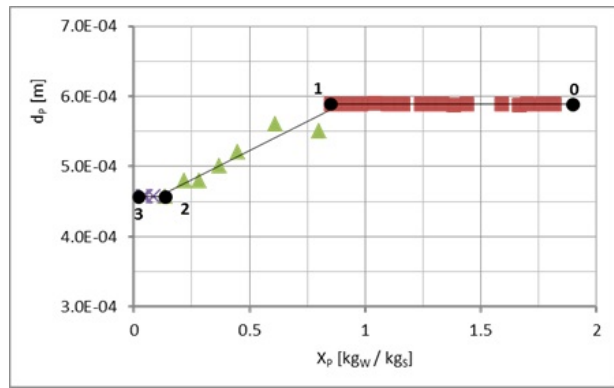


FIGURE 5. The dependence of mean particle diameter on particle absolute humidity.

### 3.3. THE DRYING RATE IN THE POROUS LAYER PERIOD

The porous layer period is defined for section 0–1 in Fig. 1. The porosity of the dried particles layer was determined according to the formula for a porous layer [14]

$$\varepsilon_{01} = \varepsilon_0 + 0.33 \frac{d_{P_{01}}}{D_k}, \quad (14)$$

where  $\varepsilon_0$ , as the probable mean porosity value, is within the interval  $\varepsilon_0 = 0.38$  to  $0.39$  [11]. The mean ion exchanger particle diameter in the studied area is  $d_{P_{01}}$ , and  $D_k$  is the diameter of the fluid dryer column. If you introduce porosity  $\varepsilon_{01}$  and mean particle diameter  $d_{P_{01}}$  into the equation (13), you will obtain the specific surface of particles  $a_{s_{01}}$  in this studied period. The total particle volume  $V_{P_{01}}$  is determined using equation (12), where  $m_s$  is the mass of the dry particles and  $\rho_{SW_1}$  is the density of the wet particles at the final point of the studied area, i.e., at point 1 in Fig. 1 and Fig. 2. This value is determined using equation (9), where  $\rho_S$  is the density and  $m_s$  is the mass of the dry particles. The mass of the moisture or of the dried water in this area is expressed by  $m_{W_{01}}$ . If we introduce the specific surface of particles  $a_{s_{01}}$  and the total particle volume  $V_{P_{01}}$  into the equation (11), we will obtain  $A_{S_{01}}$ , i.e., the total surface of the dried particles in this period.

The drying rate in the porous layer period  $N_{W_{01}}$  is determined using equation (10), where  $m_s$  is the mass of the dry particles and  $A_{S_{01}}$  is the total surface of the dried particles. Quantity  $\Delta X_{W_{01}}$  is the difference in absolute moisture of the dried particles between the initial point and the final point of the studied period and  $\Delta \tau_{01}$  is the length of this period. Table 2 summarizes the determined values of characteristic quantities for this period of the drying process of particles of the regenerated ion exchanger for individual diameters of drying columns.

### 3.4. THE DRYING RATE IN THE FIRST PERIOD OF FLUIDIZED-BED DRYING

In the region of the first period of fluidized-bed drying (period 1–2 in Fig. 1) the transition of the particles to the fluidized state begins and moisture from the particle

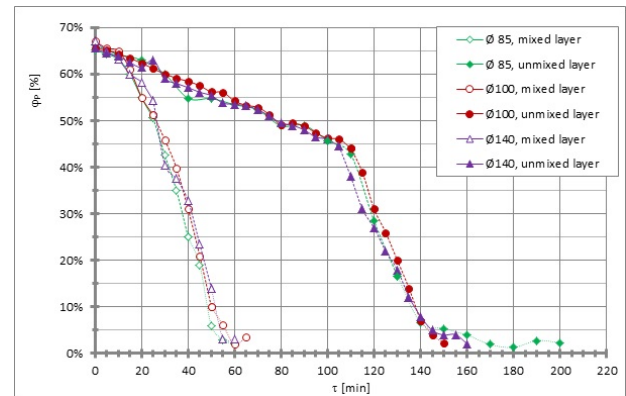


FIGURE 6. Resulting drying curves.

centre starts to evaporate. This causes a change in the particle diameter, which depends on the moisture of the particle (see Fig. 5). There are important values for determining the properties of the fluidized-bed layer, namely the velocity at the fluidization threshold  $u_{A,mf}$  and the porosity  $\varepsilon_{12}$  at superficial drying air velocity  $u_{AB}$ . The rate at the fluidization threshold is determined using the following formula:

$$u_{A,mf} = \frac{Re_{P,mf} \mu_{AB}}{d_{P_{12}} \rho_{AB}}, \quad (15)$$

where  $\mu_{AB}$  is the dynamic viscosity and  $\rho_{AB}$  is the density of the drying air. Variable  $d_{P_{12}}$  represents the mean particle diameter in this studied period. To determine the velocity at the fluidization threshold  $u_{A,mf}$ , quantity  $Re_{P,mf}$  must be determined in advance [15] according to the formula in the period valid for fine particles

$$Re_{P,mf} = (33.7^2 + 0.0408Ar)^{0.5} - 33.7, \quad (16)$$

where the Archimedes number  $Ar$  is defined by equation (8). This is determined by the dynamic viscosity  $\mu_{AB}$ , the density of the drying air  $\rho_{AB}$ , the acceleration of gravity  $g$ , the mean particle diameter  $d_{P_{12}}$  and the final particle density  $\rho_{SW_{12}}$  in the calculated period 1–2. This value is determined according to equation (9), where  $m_S$  is the dry mass of the particles,  $\rho_S$  is the density of the dry particles and value  $m_{W_{12}}$  is given by the average mass of the particle moisture for the studied period.

The porosity for the first period of fluidized-bed drying  $\varepsilon_{12}$  is also determined using formula (7), where  $Ar$  is the Archimedes number for this period and  $Re$  is the Reynolds number determined at the superficial drying air velocity  $u_{AB}$ , the dynamic viscosity  $\mu_{AB}$  and the density  $\rho_{AB}$  of drying air in the period  $B$  in Fig. 3.

The drying rate for the first period of fluidized-bed drying is determined according to formula (10), where  $m_S$  represents dry material mass and  $A_{s_{12}}$  is the total area of dried particles determined using formulas (11), (12), (13) and (9) for the studied periods. An overview of the values of characteristic quantities for this period

Column diameter	$D_k$	m	0.085	0.100	0.140
<b>Stirred version</b>					
Mean value of particle size	$d_{P_{01}}$	m	$5.9 \cdot 10^{-4}$	$5.9 \cdot 10^{-4}$	$5.9 \cdot 10^{-4}$
Period time	$\Delta\tau_{01}$	s	1634	1625	1860
Difference in humidity	$\Delta X_{W_{01}}$	$\text{kg}_W \text{kg}_S^{-1}$	0.962	1.125	1.030
Water mass at point 0	$m_{W_0}$	kg	0.227	0.306	0.533
Water mass at point 1	$m_{W_1}$	kg	0.122	0.165	0.287
Water mass at period 0–1	$m_{W_{01}}$	kg	0.105	0.141	0.246
Density of wet particles at point 1	$\rho_{s_1}$	$\text{kg m}^{-3}$	2880	2880	2880
Mean value of porosity	$\varepsilon_0$	–	0.39	0.39	0.39
Porosity	$\varepsilon_{01}$	–	0.39	0.39	0.39
Specific surface of particles	$a_{s_1}$	$\text{m}^{-1}$	6207	6210	6216
Total particle volume	$V_{P_1}$	$\text{m}^3$	$4.54 \cdot 10^{-5}$	$5.61 \cdot 10^{-5}$	$9.79 \cdot 10^{-5}$
Total surface of particles	$A_{s_1}$	$\text{m}^2$	0.28	0.35	0.61
Drying rate	$N_{w_{01}}$	$\text{kg m}^{-2} \text{s}^{-1}$	$2.55 \cdot 10^{-4}$	$3.27 \cdot 10^{-4}$	$2.61 \cdot 10^{-4}$
<b>Unstirred version</b>					
Mean value of particle size	$d_{P_{01}}$	m	$5.9 \cdot 10^{-4}$	$5.9 \cdot 10^{-4}$	$5.9 \cdot 10^{-4}$
Period time	$\Delta\tau_{01}$	s	5687	5880	5765
Difference in humidity	$\Delta X_{W_{01}}$	$\text{kg}_W \text{kg}_S^{-1}$	1.035	1.018	1.003
Water mass at point 0	$m_{W_0}$	kg	0.220	0.327	0.571
Water mass at point 1	$m_{W_1}$	kg	0.097	0.144	0.251
Water mass at period 0–1	$m_{W_{01}}$	kg	0.123	0.183	0.319
Density of wet particles at point 1	$\rho_{s_1}$	$\text{kg m}^{-3}$	2618	2618	2618
Mean value of porosity	$\varepsilon_0$	–	0.39	0.39	0.39
Porosity	$\varepsilon_{01}$	–	0.39	0.39	0.39
Specific surface of particles	$a_{s_1}$	$\text{m}^{-1}$	6207	6210	6216
Total particle volume	$V_{P_1}$	$\text{m}^3$	$3.85 \cdot 10^{-5}$	$5.87 \cdot 10^{-5}$	$1.03 \cdot 10^{-4}$
Total surface of particles	$A_{s_1}$	$\text{m}^2$	0.24	0.36	0.64
Drying rate	$N_{w_{01}}$	$\text{kg m}^{-2} \text{s}^{-1}$	$9.02 \cdot 10^{-5}$	$8.35 \cdot 10^{-5}$	$8.38 \cdot 10^{-5}$

TABLE 2. Overview of values for determination of drying rate in the porous layer period.

of the drying process of particles of the regenerated ion exchanger is summarized in Table 3.

### 3.5. EFFECT OF THE STIRRER ON THE TOTAL DRYING TIME

A comparison of the drying curves for the stirred and unstirred fluidized bed layers is shown in Fig. 6. A comparison of these curves shows the effect of the stirrer on the porous layer area, where the drying time is significantly shorter. The rotating stirrer also helps the particles pass to the fluid state already at 50 % RH instead of the initial 45 % RH. There is also a positive effect of the stirrer on the first period of fluidized-bed drying, because it sweeps the wet par-

ticles stuck on the walls back into the fluidized-bed layer, where the transfer phenomena are more intensive.

## 4. CONCLUSIONS

It has been demonstrated that the stirrer has a positive effect on the porous layer period and during the first period of the drying process in the fluidized bed layer. The stirrer regularly disturbs the stationary porous layer that has formed, and this intensifies the rate of the transport phenomena. The total drying time to reach the required moisture content of the material is thus 60 minutes, which corresponds to a 63 % shorter drying time.

Column diameter	$D_k$	m	0.085	0.100	0.140
<b>Stirred version</b>					
Mean value of particle size	$d_{P_{12}}$	m	$5.30 \cdot 10^{-4}$	$5.30 \cdot 10^{-4}$	$5.30 \cdot 10^{-4}$
Period time	$\Delta\tau_{12}$	s	1434	1262	1587
Difference in humidity	$\Delta X_{W_{12}}$	$\text{kg}_W \text{kg}_S^{-1}$	0.588	0.588	0.588
Water mass at point 1	$m_{W_1}$	kg	0.122	0.165	0.287
Water mass at point 2	$m_{W_2}$	kg	0.022	0.029	0.051
Water mass at period 1-2	$m_{W_{12}}$	kg	0.100	0.136	0.236
Density of wet particles at point 2	$\rho_{SW_2}$	$\text{kg m}^{-3}$	2290	2070	1802
Archimedes number	$Ar$	–	6046	5465	4756
Reynolds number of fluidization threshold	$Re_{p,mf}$	–	3.480	3.160	2.766
Rate at fluidization threshold	$u_{A,mf}$	$\text{m s}^{-1}$	0.16	0.15	0.13
Porosity at fluidization start	$\varepsilon_{mf}$	–	0.40	0.40	0.40
Reynolds number at $u_{AB}$	$Re$	–	43	47	44
Porosity at working conditions	$\varepsilon_{12}$	–	0.79	0.82	0.83
Specific surface of particles	$a_{s_{12}}$	$\text{m}^{-1}$	2429	2016	1930
Total particle volume	$V_{p_{12}}$	$\text{m}^3$	$8.47 \cdot 10^{-5}$	$1.14 \cdot 10^{-4}$	$1.99 \cdot 10^{-4}$
Total surface of particles	$A_{s_{12}}$	$\text{m}^2$	0.21	0.23	0.38
Drying rate	$N_{w_{12}}$	$\text{kg m}^{-2} \text{s}^{-1}$	$2.43 \cdot 10^{-4}$	$3.33 \cdot 10^{-4}$	$2.76 \cdot 10^{-4}$
<b>Unstirred version</b>					
Mean value of particle size	$d_{P_{12}}$	m	$5.30 \cdot 10^{-4}$	$5.30 \cdot 10^{-4}$	$5.30 \cdot 10^{-4}$
Period time	$\Delta\tau_{12}$	s	1406	1411	1691
Difference in humidity	$\Delta X_{W_{12}}$	$\text{kg}_W \text{kg}_S^{-1}$	0.497	0.497	0.497
Water mass at point 1	$m_{W_1}$	kg	0.097	0.144	0.251
Water mass at point 2	$m_{W_2}$	kg	0.021	0.031	0.054
Water mass at period 1-2	$m_{W_{12}}$	kg	0.076	0.113	0.197
Density of wet particles at point 2	$\rho_{SW_2}$	$\text{kg m}^{-3}$	2315	2030	1778
Archimedes number	$Ar$	–	6114	5359	4693
Reynolds number of fluidization threshold	$Re_{p,mf}$	–	3.517	3.101	2.730
Rate at fluidization threshold	$u_{A,mf}$	$\text{m s}^{-1}$	0.16	0.14	0.13
Porosity at fluidization start	$\varepsilon_{mf}$	–	0.40	0.40	0.40
Reynolds number at $u_{AB}$	$Re$	–	43	47	44
Porosity at working conditions	$\varepsilon_{12}$	–	0.78	0.83	0.83
Specific surface of particles	$a_{s_{12}}$	$\text{m}^{-1}$	2450	1977	1904
Total particle volume	$V_{p_{12}}$	$\text{m}^3$	$8.22 \cdot 10^{-5}$	$1.22 \cdot 10^{-4}$	$2.13 \cdot 10^{-4}$
Total surface of particles	$A_{s_{12}}$	$\text{m}^2$	0.20	0.24	0.41
Drying rate	$N_{w_{12}}$	$\text{kg m}^{-2} \text{s}^{-1}$	$2.08 \cdot 10^{-4}$	$2.57 \cdot 10^{-4}$	$2.22 \cdot 10^{-4}$

TABLE 3. Overview of values for determination of drying rate in the first period of fluidized-bed drying

It follows from the experiments and the results that the drying rate in the period of the porous stationary layer is  $8.58 \cdot 10^{-5} \text{ kg m}^{-2} \text{ s}^{-1} \pm 5\%$ , and after introducing the stirrer the rate increases to  $2.81 \cdot 10^{-4} \text{ kg m}^{-2} \text{ s}^{-1} \pm 16\%$ , which represents an increase of 220%.

In the first and second periods of fluidized-bed drying, the stirrer does not disturb the fluidized bed layer that has formed. Then intensification of the process helps, and the stuck wet particles are swept off the walls of the drying chamber into the fluidized bed. This results in an increase in the drying rate in the first period of fluidized-bed drying from  $2.29 \cdot 10^{-4} \text{ kg m}^{-2} \text{ s}^{-1} \pm 12\%$  to  $2.84 \cdot 10^{-4} \text{ kg m}^{-2} \text{ s}^{-1} \pm 17\%$ , i.e. an increase of 17%.

The results presented here are based on more than one hundred long-term drying experiments resulting in figures that provide a description of the course of investigated drying process.

#### ACKNOWLEDGEMENTS

The authors appreciate the support provided by internal grant SGS12/057/OHK2/1T/12 of the Czech Technical University in Prague, grant INGO LG 13036 of the Czech Ministry of Education, and research project J04/98: 212200008 of the Czech Ministry of Education.

#### LIST OF SYMBOLS

$D_k$	Column diameter [m]
$Ar$	Archimedes number [-]
$a_s$	Specific surface of particles [ $\text{m}^{-1}$ ]
$A_S$	Total surface of particles [ $\text{m}^2$ ]
$C_8-C_{11}$	Calculation constants [-]
$d$	Diameter [m]
$g$	Acceleration of gravity [ $\text{m s}^{-2}$ ]
$h$	Height [m]
$m$	Mass [kg]
$n$	Amount of substance [mol]
$N_w$	Drying rate [ $\text{kg m}^{-2} \text{ s}^{-1}$ ]
$p$	Pressure [Pa]
$p''$	Pressure of saturated water vapours [Pa]
$R$	Universal gas constant [ $\text{J K}^{-1} \text{ mol}^{-1}$ ]
$Re$	Reynolds number [-]
$S$	Cross-section [ $\text{m}^2$ ]
$t$	Temperature [ $^{\circ}\text{C}$ ]
$T$	Thermodynamic temperature [K]
$u$	Velocity [ $\text{m s}^{-1}$ ]
$V$	Total particle volume [ $\text{m}^3$ ]
$\bar{V}$	Volume flow [ $\text{m}^3 \text{ s}^{-1}$ ]
$X$	Absolute humidity (moisture) [ $\text{kg}_w \text{ kg}_s^{-1}$ ]
$\varepsilon$	Porosity [-]
$\varphi$	Relative humidity (moisture) [% RH (RM)]
$\mu$	Viscosity [Pa s]
$\rho$	Density [ $\text{kg m}^{-3}$ ]
$\tau$	Time period [s]

#### LIST OF SUBSCRIPTS

$A$	Air
$W$	Water (humidity, moisture)
$SW$	Wet material
$S$	Dry matter
$P$	Particle
$m$	Stirrer
$K$	Column
0	Initial point
1	Transition point between the periods of the porous layer and the first period of fluidized-bed drying
2	Transition point between the periods of the first and second period of fluidized-bed drying
$A$	Zone of cold air
$B$	Zone of heated air
$C$	Zone of chilled wet air
$WALL$	Wall

#### REFERENCES

- [1] Kim J, Han G.Y.: Effect of agitation on fluidation characteristics of fine particles in a fluidized bed. *Powder Technol.* 2006; 166:113-122  
DOI: 10.1016/j.powtec.2006.06.001
- [2] Daud W.R.W.: Fluidized bed dryers - recent advances. *Adv. Powder Technol.* 2008; 19:403-418  
DOI: 10.1163/156855208X336675
- [3] Ying Han, Jia-Jun Way, Xue-Ping Gu, Lian-Fang Feng, Guo-Hua Hu.: Homogeneous Fluidization of Geldart D particles in a Gas-Solid Fluidized Bed with a Frame Impeller. *Industrial & Engineering Chemistry Research.* 2012; 51(50) 16482-16487 DOI: 10.1021/ie301574q
- [4] Ying Han, Jia-Jun Way, Xue-Ping G.U., Lian-Fang Feng, Guo-Hua Hu.: Effect of Agitation on the Fluidization Behavior of a Gas-Solid Fluidized Bed with a Frame Impeller. *AIChE Journal.* 2013;59: 1066-1074.  
DOI: 10.1002/aic.13893
- [5] Mega.cz, RALEX heterogenous ionex membranes (in Czech). QARTIN s.r.o., [Online]. Available: <http://www.mega.cz/heterogenni-iontomenicove-membrany-ralex.html> [Approach obtained 20 11 2012].
- [6] M. J. Hudson, P. A. Williams.: *Recent Developments in Ion Exchangers, Ion Exchangers in the Nuclear Industry.* Springer Netherlands. 1990.
- [7] L. Jelínek.: *Desalination and separation methods in water treatment (in Czech).* Prague Institute of Chemical Technology. 2009.
- [8] Dow, DoweX marathon A, 26 11 2010. [Online]. Available: [http://www.dowwaterandprocess.com/products/ix/dx\\_mar\\_a.htm](http://www.dowwaterandprocess.com/products/ix/dx_mar_a.htm) [Approach obtained 22 05 2011].
- [9] J. Chyský.: *Moist air (in Czech).* Publishing House of the Czech Technical University in Prague. 1977.
- [10] J. Šesták, J. Bukovský and M. Houška.: *Thermal Processes: Transport and thermodynamic data (in Czech).* Publishing House of the Czech Technical University in Prague. 1993.
- [11] S. H. Touloukian.: *Thermophysical properties of matter, sv. 11.* IFI/Plenum Press, 1975.

- [12] R. T. Goroško. *Izv. Vuzov. Neft i gaz.*: 1958;1:125.
- [13] A. S. Mujumdar.: *Handbook of Industrial Drying*. Dekker. 1995.
- [14] V. Hlavačka.: *Thermal processes in technical systems of gas-solid particles (in Czech)*. Publishing House of Technical Literature. 1980.
- [15] C. Wen and Y. Yu.: A generalized method for predicting the minimum fluidization velocity. *AICHE Journal*. 1966; 12:610-612.